



Published in final edited form as:

Exp Neurol. 2015 February ; 264: 82–91. doi:10.1016/j.expneurol.2014.12.008.

Early hyperactivity in lateral entorhinal cortex is associated with elevated levels of A β PP metabolites in the Tg2576 mouse model of Alzheimer's disease

Wenjin Xu^{1,2}, Shane Fitzgerald^{1,3}, Ralph A. Nixon^{3,4,5}, Efrat Levy^{3,4,6}, and Donald A. Wilson^{1,2,7}

¹Emotional Brain Institute

³Center for Dementia Research, Nathan S. Kline Institute for Psychiatric Research, Orangeburg, NY, 10962

²Departments of Child & Adolescent Psychiatry

⁴Psychiatry

⁵Cell Biology

⁶Biochemistry and Molecular Pharmacology

⁷Neuroscience and Physiology, New York University School of Medicine, New York, NY, 10016

Abstract

Alzheimer's disease (AD) is a neurodegenerative disorder that is the most common cause of dementia in the elderly today. One of the earliest symptoms of AD is olfactory dysfunction. The present study investigated the effects of amyloid β precursor protein (A β PP) metabolites, including amyloid- β (A β) and A β PP C-terminal fragments (CTF), on olfactory processing in the lateral entorhinal cortex (LEC) using the Tg2576 mouse model of human A β PP over-expression. The entorhinal cortex is an early target of AD related neuropathology, and the LEC plays an important role in fine odor discrimination and memory. Cohorts of transgenic and age-matched wild-type (WT) mice at 3, 6, and 16 months of age (MO) were anesthetized and acute, single-unit electrophysiology was performed in the LEC. Results showed that Tg2576 exhibited early LEC hyperactivity at 3 and 6 MO compared to WT mice in both local field potential and single-unit spontaneous activity. However, LEC single-unit odor responses and odor receptive fields showed no detectable difference compared to WT at any age. Finally, the very early emergence of olfactory system hyper-excitability corresponded not to detectable A β deposition in the olfactory system, but rather to high levels of intracellular A β PP-CTF and soluble A β in the anterior piriform cortex (aPCX), a major afferent input to the LEC, by 3 MO. The present results add to the growing

© 2014 Elsevier Inc. All rights reserved.

Address for correspondence: Donald Wilson, EBI, Nathan Kline Institute, 140 Old Orangeburg Road, Orangeburg, NY 10962 USA, phone 845-398-2178; dwilson@nki.rfmh.org.

Publisher's Disclaimer: This is a PDF file of an unedited manuscript that has been accepted for publication. As a service to our customers we are providing this early version of the manuscript. The manuscript will undergo copyediting, typesetting, and review of the resulting proof before it is published in its final citable form. Please note that during the production process errors may be discovered which could affect the content, and all legal disclaimers that apply to the journal pertain.

evidence of A β PP-related hyper-excitability, and further implicate both soluble A β and non-A β A β PP metabolites in its early emergence.

Keywords

Lateral entorhinal cortex; olfaction; Alzheimer's Disease; single-unit; A β PP metabolites; amyloid- β ; A β PP C-terminal fragments

Introduction

Amyloid- β (A β) deposition and neurofibrillary tangles (NFTs) have long been implicated as hallmarks of AD pathology (Hardy and Higgins, 1992, Ittner and Gotz, 2011, Selkoe, 1994). A β has been shown to exist in a number of different forms including soluble A β monomers and oligomers, as well as insoluble protofibrils and A β plaques (Walsh, et al., 1999, Walsh, et al., 1997, Walsh and Selkoe, 2007). However, the correlation between A β pathology and cognitive decline in humans is variable, particularly in pre-depositing stages of the disease (Cummings and Cotman, 1995, Goutagny, et al., 2013). Amyloid β precursor protein (A β PP) is processed by α - and β -secretases. Cleavage by the latter results in a β C-terminal fragment (β CTF) that contains the A β domain and generates A β and A β PP intracellular cytoplasmic domain when further processed by γ -secretase (Zheng and Koo, 2006, Zheng and Koo, 2011). The human A β PP metabolites A β and A β PP-CTF have been shown to exhibit some level of cytotoxicity in the pre-depositing brain, ranging from inducing endosome anomalies and apoptosis (Bertrand, et al., 2001, Cheng, et al., 2013, Deyts, et al., 2012, Jiang, et al., 2010, Kaye, et al., 2003, Lauritzen, et al., 2012, Lu, et al., 2000, McPhie, et al., 2001, Nhan, et al., 2014, Tamayev and D'Adamio, 2012, Tamayev, et al., 2012, Upadhaya, et al., 2012) to causing abnormal rewiring of neurons (Cheng, et al., 2011) and functional disruption of synapses (Lacor, et al., 2004).

The effect of A β PP and its metabolites on the olfactory system and resulting consequences for odor processing are of particular interest given that olfactory dysfunction is one of the most commonly reported early symptoms of AD and other neurodegenerative diseases (Wilson, et al., 2014). This dysfunction has been shown to precede other cognitive impairments and although it can manifest as deficits in the detection and discrimination of odors in mild cognitive impairment and early AD (Bahar-Fuchs, et al., 2011, Murphy, 1999, Rahayel, et al., 2012), problems with odor identification appear most robust (Albers, et al., 2006, Calhoun-Haney and Murphy, 2005, Conti, et al., 2013, Devanand, et al., 2008, Devanand, et al., 2000, Rahayel, et al., 2012).

The early appearance of olfactory deficits may be linked to the fact that the entorhinal cortex that is one of the first brain regions to display AD related pathology (Braak and Braak, 1996, Braak, et al., 2011) serves at least two roles in olfactory perception and memory. The lateral entorhinal cortex (LEC) receives direct input from the olfactory bulb and piriform cortex (Cleland and Linstner, 2003, Igarashi, et al., 2012). This information is then projected to the hippocampal formation via the perforant path for hippocampal-dependent odor memory (Staubli, et al., 1984). In addition, the LEC projects back to both the olfactory bulb and piriform cortex (Chapuis, et al., 2013). This top-down pathway is critical for fine odor

discrimination (Chapuis, et al., 2013), as well as modulating piriform cortical odor responses (Chapuis, et al., 2013, Mouly and Di Scala, 2006), and non-hippocampal dependent odor memory (Boisselier, et al., 2014, Ferry, et al., 1996, Wirth, et al., 1998).

The present study assessed the effect of mutated human A β PP overexpression and early levels of its metabolites on LEC physiology. Similar to results in the piriform cortex (Wesson, et al., 2011), Tg2576 mice showed LEC hyperexcitability which emerged prior to A β deposition. Here we demonstrate that this early, pre-A β depositing LEC hyperexcitability occurs in the presence of high levels of soluble A β and intracellular A β PP-CTF, especially in the piriform cortex, a major afferent input to the LEC.

Materials and Methods

Subjects

A total of 17 Tg2576 (n=2 female and 3 male 3 MO, n=2 female and 3 male 6 MO, n=3 female and 4 male 16 MO) and 21 age-matched B6sJLF/J WT (n=4 female and 3 male at 3, 6, and 16 MO) mice were obtained from a breeding colony at the Nathan S. Kline Institute for use in the present study for electrophysiology, histology and immunohistochemistry. All animals were recorded from within 1 week (+/-) of the specified age ranges. Animals were housed in groups of 3–4 animals per polypropylene cage until at most 4 days before recording, during which time they were separated and individually housed. Food and water was available *ad lib* unless otherwise noted. All handling, housing and experimental procedures were in accordance with the Institutional Animal Care and Use Committee guidelines at Nathan S. Kline Institute as well as NIH guidelines for the proper treatment of animals.

Acute Unit and LFP Recordings and Odorant Stimulation

Acute single-unit recording procedures in the LEC were performed similarly to Xu and Wilson, 2012. Animals were anesthetized with urethane (1.25 mg/kg). Single units were recorded with a tungsten microelectrode (1–5 Mohm) and signals were acquired and analyzed with Spike2 physiology software (CED). Units were identified and separated off-line with template matching and PCA (Spike2 software) and showed at least a 2-ms refractory period in interval histograms. LEC units (filtered 0.3–3 kHz) were identified with histological confirmation of electrode position. Electrode placement here was confirmed through evoked responses from stimulation in the OB as well as histological confirmation.

Olfactory stimuli were delivered with a flow-dilution olfactometer positioned 2 cm from the animal's nose. Odor vapor was introduced with a computer-controlled pinch valve at a rate of 0.1 liters per minute (LPM) to a constant 1 LPM flow of nitrogen gas. Stimuli were introduced for 2 s per trial with at least a 30 s inter-stimulus interval. A total of 6 odors were used (3 monomolecular, 3 odor-mixtures). Each odor was presented randomly for 4 trials for each single-unit recording. The monomolecular odorants used were ethyl valerate, isoamyl acetate and heptanal. The odor-mixtures used have been previously described (Barnes, et al., 2008, Chapuis and Wilson, 2012, Lovitz, et al., 2012, Xu and Wilson, 2012). As noted in these publications, 10C is a mixture comprised of 10 different monomolecular odors, 10C-1

is the same mixture as 10C with one component removed, and 10CR1 is the same mixture as 10C with one component replaced with a different component. The component removed in 10C-1 and replaced in 10CR1 were consistent across animals and throughout the present experiment. Both pure odorants and mixtures were diluted in mineral oil to a concentration of 100 ppm based on vapor pressure. As a result, mixtures had a higher concentration than pure monomolecular odorants.

Data Analysis

Single-unit and LFP data were all analyzed with Spike2 (CED, Inc). Single units were identified with principal components analyses as well as templating. Recordings were identified as coming from a single-unit by confirming a minimum 2 ms refractory period using interval histograms. Single-unit odor-evoked activity was defined as the spike count 3 s after stimulus onset with basal firing rate (3 s pre-stimulus onset) subtracted. Odor-evoked responses were normalized to the maximal odor response (best odor) of a cell to obtain a relative response magnitude to each odor by each neuron. Spontaneous activity was defined as the per second spike rate 3 s before stimulus onset.

LFP responses were investigated in the theta (7–12 Hz), beta (15–35 Hz) and gamma (40–80 Hz) frequency bands. Spontaneous power was defined as the activity 3 s before stimulus onset. Odor-evoked power was defined as the activity 3 s after stimulus onset. Odor-evoked and spontaneous power was averaged across the 6 odorants to obtain one set of evoked and spontaneous LFP power per frequency bands per animal.

In addition to odor responses, single-unit entrainment to LFP beta oscillations were analyzed. This was done by first extracting a time stamp for each beta oscillatory wave. Negative oscillatory peaks were extracted from the beta frequency filtered LFP by thresholding at two times the standard deviation of the filtered signal. Phase plots of single-unit activity were constructed relative to these peak events and analyzed with Rayleigh statistics using MatLab sub-routines for circular statistics called CircStat (Berens, 2009). MatLab was used to conduct Rayleigh statistics on entrainment data. A Chi-square test was employed to check for significance between genotypes.

All statistical comparisons were done using StatView. Two-way repeated measures ANOVAs were used to compare single-unit odor-evoked receptive fields. Two-way between groups ANOVAs were used to compare spontaneous and odor-evoked LFP power in the theta, beta, and gamma frequencies and spontaneous and maximal evoked single-unit activity. T-tests and post-hoc Fisher's tests were used where appropriate to make pair-wise comparisons.

Histology

After recording, mice were overdosed with urethane and transcardially perfused with PBS and 4% paraformaldehyde/PBS. Brains were removed and post-fixed in 30% sucrose/4% paraformaldehyde. Coronal brain sections (40 μ m) were cut using a sliding microtome (Leica). A portion of these were mounted and stained with cresyl violet for electrode verification (Fig. 1). The remainder sections were stored as floating sections in 0.2% sodium azide/PBS for thioflavin S staining and for immunohistochemistry. Coronal sections were

stained with thioflavin S as previously described in (Wesson, et al., 2010). Briefly, tissue samples were mounted and allowed to dry before immersion in 1% thioflavin S (Sigma-Aldrich). These were then rehydrated through immersion in increasing concentrations of ethanol before rinsing with dH₂O and cover slipped. Staining groups always included sections from each age group and genotype.

Immunohistochemistry

Coronal sections were immunolabeled with the antibodies 6E10, C1/6.1 or 22C11 as previously described in (Wesson, et al., 2010). Briefly, sections were rinsed and blocked for 1 hour with 20% filtered normal goat serum diluted in PBS. Sections were then incubated in 6E10 (1:200), C1/6.1 (1:200) or 22C11 (1:100) or buffer overnight at 4°C. Sections were rinsed with PBS and incubated for 2 hours in Alexafluor488 anti-mouse secondary antibody (1:500). After incubation, tissue was rinsed a final time, mounted onto glass slides, dried and covered using GelMount. Immunolabeled groups always included sections from each age group and genotype.

Western Blot

A separate group of 3 MO (n=3 females and 1 male WT, n=4 females Tg2576), 6 MO (n=2 females WT, n=2 females Tg2576), and 12 MO (n=3 females and 1 male WT, n=4 females Tg2576) mice were anesthetized with isoflurane and sacrificed. Brains were removed, placed on ice and bilateral OB, PCX, HPX, LEC and cerebellum were dissected out for western blot analysis.

Methods were adapted from (Morales-Corraliza, et al., 2013). Brain tissue was homogenized in THB (1 ml/100 mg of sample) [1M Tris base (pH 7.4)] and frozen (-80°C) overnight. Protein concentration was determined by BCA Protein Assay Kit. Equal amounts of total protein (20 µg for AβPP-CTF and full-length AβPP (flAβPP, 40 µg for Aβ) were loaded on a 4–20% Tris glycine SDS gel (SDS-PAGE), separated electrophoretically, and transferred onto a PVDF membrane. The membrane was washed and incubated in 5% milk in TBST for 1 hour at room temperature, followed by overnight incubation at 4°C with either C1/6.1 or 4G8 mouse antibody (1:1000) and washed in TBST before secondary antibody incubation in anti-mouse secondary antibody (1:5000) in 5% milk in TBST for 1 hour at room temperature. After a final wash in TBST, Pierce ECL Western Blotting Substrate (2 ml/blot) was employed for detection of flAβPP, and 1 ml of this solution was mixed with 1 ml of SuperSignal Western Femto Maximum Sensitivity Substrate for detection of AβPP-CTF and Aβ. Stripped membranes were blotted with anti-GAPDH antibody for internal control for loading. Densitometry analysis using ImageJ (NIH) was utilized to quantify protein bands and densities were normalized as a ratio of GAPDH.

Sandwich Enzyme-Linked Immunosorbent Assay (ELISA) for detection of Aβ

Bilateral OB, PCX, HPX, LEC and cerebellum were dissected out and tissues from two mice were combined (n=6 Tg2576 at each age group). Brain tissue was homogenized in THB as described for western blot analysis and following treatment with diethylamine (DEA) and centrifugation at 135,000 x g, levels of human Aβ were determined by sandwich ELISA as previously described (Morales-Corraliza, et al., 2009).

Results

Tg2576 mice show elevated single-unit spontaneous activity in lateral entorhinal cortex

Previous reports have shown that A β accumulation can lead to spontaneous hyperactivity at the single-unit level in neurons in close proximity to the deposits (Busche, et al., 2012, Busche, et al., 2008, Cacucci, et al., 2008, Wesson, et al., 2011). In addition, even at pre-depositing ages, these changes may already be present (Cao, et al., 2012, Guerin, et al., 2009). In order to investigate this phenomenon, a total of 58 single-units for Tg2576 mice (n=19 3 MO, n=21 6 MO, n=18 16 MO) and 70 units for WT mice (n=23 3 MO, n=26 6 MO, n=21 16 MO) were recorded in LEC (Fig. 1). Spontaneous activity was defined as a 3 second (s) period before the onset of odor stimuli. Since there were 24 odor presentations per single-unit, these periods were averaged and divided by 3 to establish an average spikes per second rate. This revealed that Tg2576 exhibited significantly higher spontaneous activity than age-matched WT ($F(1,124) = 17.98, p < .0001$ for genotype). Further analysis confirmed that this hyperactivity was present at all ages ($t(40) = 2.79, p < .01$ for 3 MO, $t(45) = 2.61, p < .05$ for 6 MO, $t(39) = 2.12, p < .05$ for 16 MO) (Fig. 2A).

Tg2576 mice show no change in single-unit receptive fields in lateral entorhinal cortex

Previous work has demonstrated that single-unit odor receptive fields are reflective of olfactory sensory acuity (Barnes, et al., 2008, Chapuis and Wilson, 2012, Chen, et al., 2011). Thus, as a first investigation into olfactory processing in the presence of A β PP overexpression, we examined receptive fields of units in LEC of Tg2576. As defined in (Xu and Wilson, 2012), receptive fields were calculated by taking the average firing rate of single-units to 4 random presentations of a single odorant and normalizing this rate to the best of 6 different odorants. Odor-evoked firing was defined as the firing rate 3 seconds after the onset of an odor stimulus. Maximal odor-evoked activity to the 'best' odorant did not differ between Tg2576 and WT LEC neurons ($F(1, 124) = 0.00, p = \text{N.S.}$) (Fig. 2B). Receptive field measures revealed no significant difference between Tg2576 and WT within any age group ($F(1,124) = 2.48, p = \text{N.S.}$) suggesting that there was no difference in the odor-evoked acuity of single-units in LEC between genotypes (Fig. 3).

Tg2576 mice show hyper-excitable spontaneous and odor-evoked LFP oscillations in early life that persist in later life

While single-unit recordings are a measure of the activity level of a single-neuron within a population of cells, LFPs offer an opportunity to assess the aggregate network activity of that population. We have previously reported elevated LFP oscillatory activity in OB and piriform cortex of young Tg2576 mice (Wesson, et al., 2011). Here, a similar effect is apparent in LEC LFPs. Elevated baseline ($F(1,150) = 29.09, p < .0001$) as well as odor-evoked activity ($F(1,150) = 38.52, p < .0001$) was apparent in Tg2576 vs. WT at 3 months of age (Fig. 4A). This persisted in the 6 MO group (Fig. 4B) of animals ($F(1,150) = 11.01, p < .005$ for baseline, $F(1,150) = 13.07, p < .0005$ for evoked). Both baseline ($F(1,165) = 14.35, p < .0005$) and odor-evoked activity ($F(1,165) = 8.92, p < .005$) remained hyperactive compared to WT even in the oldest (16 MO) animals (Fig. 4C).

A β deposition is elevated in 16 MO Tg2576 mice

To confirm the phenotypic development of A β pathology in the animals in the present study, staining for plaques (thioflavin S) and immunohistochemistry for A β deposition (6E10) was conducted. 3 and 6 MO Tg2576 mice showed no staining for plaques or A β deposition in any brain region examined. This varies with our previous reports of early A β deposition in the OB glomerular layer at 3 MO (Wesson, et al., 2010). We believe this discordance either reflects a real difference in Tg2576 cohorts or non-selective secondary antibody staining in the original report. Meanwhile 16 MO animals showed robust pathology in OB, aPCX, HPX as well as LEC (Fig. 5). Due to these findings, A β PP metabolite immunohistochemistry focused on the 3 and 6 MO pre-plaque stages of pathology development.

A β PP metabolites are elevated in pre-depositing Tg2576 mice

Tg2576 mice showed elevated single-unit baseline activity and elevated LFP excitability in LEC during ages 3–6 months in which A β immunostaining is not different from age-matched WT (data not shown). The absence of detectable A β immunostaining at 3–6 MO was confirmed by Western blot analysis with 4G8 (Fig. 6A). ELISA analysis of non-fibrillar, soluble A β revealed different levels of both A β 40 and A β 42 in different brain regions (Fig. 6B and 6C). The highest levels of both peptides were found in the aPCX, while very low levels were observed in the cerebellum. The ELISA data show an increase in A β levels from 3 to 6 months of age only in the LEC for both A β 42 and A β 40 (t-test 3 MO vs. 6 MO, A β 42 $t(4) = 3.66, p < 0.05$; A β 40, $t(4) = 3.95, p < 0.05$). Western blot analysis with 4G8 shows initial accumulation of A β at 12 MO only in the aPCX and the LEC (Fig. 6A). No other region showed age-dependent changes in A β levels at these ages. These data suggest a difference in the level of A β PP processing or A β clearance in different brain regions, resulting in different levels of A β . These data suggest a difference in either the level of A β PP processing or A β clearance in different brain regions, resulting in different levels of A β .

Work from other groups shows that hyperactivity at early ages in the absence of A β plaques is correlated intracellular β CTF accumulation (Cavanagh, et al., 2013). As such, we hypothesized that flA β PP overexpression, the enhanced generation of A β PP-CTFs, and/or the decreased degradation of A β PP-CTFs may be a better predictor of network hyperactivity during early life. Human A β PP overexpression in Tg2576 mice was revealed by immunoreaction with the antibody 22C11 that interacts with flA β PP and the soluble amino-terminal fragments (Fig. 7). However, a more pronounced staining is seen when Tg2576 sections were treated with the C1/6.1 antibody that reacts with flA β PP and A β PP-CTFs, suggesting enhanced intracellular levels of A β PP-CTFs in the olfactory cortical areas (OB, aPCX, LEC) as well as hippocampus (Fig. 7).

Western blot analysis with the A β PP-C-terminal C1/6.1 antibody in 3, 6, and 12 MO age cohorts revealed that Tg2576 overexpressed flA β PP ($F(1,40) = 225.07, p < .0001$) and had significantly elevated A β PP-CTFs ($F(1,40) = 213.87, p < .0001$) compared to endogenous levels in WT mice (Fig. 6A). Furthermore, this elevation is present at the early 3 MO ($F(1,30) = 143.75, p < .0001$ for A β PP-CTFs and $F(1,30) = 148.44, p < .0001$ for flA β PP) as well as 6 MO ($F(1,10) = 99.34, p < .0001$ for A β PP-CTFs and $F(1,10) = 295.54, p < .0001$ for

flA β PP) age groups. flA β PP was quantified (data not shown) and no significant differences between brain regions were found, ruling out the possibility that regional differences in A β PP-CTF levels are due partly or completely to differences in human A β PP transgene expression arising from the hamster prion protein promoter driving strong expression of the transgene in specific olfactory pathway regions. Western blot analyses for A β PP-CTFs (C1/6.1) demonstrated elevation of the human transgenic A β PP-CTF in Tg2576 in all brain regions examined compared to the endogenous fragment in age-matched WT, with no age-dependent changes (Fig. 6A and 6D). However, higher A β PP-CTFs levels were found in the aPCX than in HPX, LEC, and OB, and the lowest found in the cerebellum (repeated measures ANOVA, region x age, main effect of region, $F(4,16) = 6.48, p < 0.01$. Post-hoc Fisher tests revealed aPCX levels were significantly ($p < 0.05$) higher than all other areas. No significant main effect of age). This difference in A β PP-CTFs levels occurs already at 3 months of age (Fig. 6D). Quantification of A β PP-CTF levels relative to flA β PP confirmed the regional differences in A β PP-CTF levels, independent of flA β PP level of expression, with significantly higher A β PP-CTFs levels relative to flA β PP in the aPCX as compared to all other brain regions tested at both 3 MO and 6 MO (3 MO ANOVA, $F(4,15) = 10.06, p < 0.001$; 6 MO ANOVA, $F(4,5) = 24.63, p < 0.01$. Post-hoc Fisher tests revealed aPCX A β PP-CTF/flA β PP levels were higher in aPCX than all other areas at both ages; data not shown). The levels of β CTF relative to total A β PP-CTF were also high in the aPCX, as well as the HPX and LEC, but not in the OB and cerebellum (repeated measures ANOVA, region x age, main effect of region, $F(4,16) = 7.50, p < 0.01$. No significant main effect of age. Post-hoc Fisher tests revealed aPCX, HPX and LEC levels were significantly ($p < 0.05$) higher than OB and CRB). The difference from a ratio of 0.50 of total A β PP-CTFs was modest in LEC, and reached significance in aPCX and HPX (e.g., 3 MO t-test versus 0.5, aPCX, $t(3) = 5.14, p = 0.01$; HPX, $t(3) = 4.37, p = 0.02$; LEC, $t(3) = 2.52, p = 0.09$; Fig. 6E).

Discussion

Although olfactory impairments can occur in many disorders, olfactory dysfunction is one of the most commonly seen deficits in pre-clinical cases of AD. This dysfunction often manifests in a variety of different ways, though increasingly, odor identification has been pinpointed as a particularly good predictor of a transition from benign aging to MCI to AD in the elderly (Albers, et al., 2006, Christen-Zaech, et al., 2003, Conti, et al., 2013, Devanand, et al., 2008, Devanand, et al., 2000, Murphy, 1999, Murphy, et al., 2002, Nordin and Murphy, 1998, Rahayel, et al., 2012). Although abilities such as odor detection involve basic olfactory sensory processing, the ability to identify and discriminate odors incorporates a decidedly higher order cognitive component (Wilson and Stevenson, 2003, Wilson and Sullivan, 2011). In the present study, we sought to investigate odor processing in higher order structures in response to A β PP pathology at the single-unit level by performing acute electrophysiological recordings in LEC in the Tg2576 mouse. The LEC is an area that has been demonstrated to play an important role in odor processing and associative memory (Chapuis, et al., 2013, Ferry, et al., 1996, Frasnelli, et al., 2010, Mouly and Di Scala, 2006, Staubli, et al., 1984, Wirth, et al., 1998, Xu and Wilson, 2012). Our results show that odor processing at the single unit level in LEC remains surprisingly robust in the face of accumulating A β PP metabolites, including A β . However, LEC single-unit spontaneous

activity was significantly elevated in Tg2576 versus WT, as were both baseline and odor-evoked LFP oscillations. This hyper-excitability emerged by at least 3 MO and remained through at least 16 MO. These findings mirror other studies that have demonstrated the effect of A β PP metabolites in inducing neurotoxic effects (Bach, et al., 2001, Bertrand, et al., 2001, Cheng, et al., 2013, Cheng, et al., 2011, Devi and Ohno, 2012, Dewachter, et al., 2002, Lu, et al., 2000, McPhie, et al., 2001, Sopher, et al., 1994, Yankner, et al., 1989). However, to the best of our knowledge, this is the first investigation of this disrupted firing activity in the LEC in response to odor stimuli.

The single-unit activity reported here demonstrates that odor processing remains largely intact in LEC of Tg2576 from early to middle-age. Although expression of mutant human A β PP in the more peripheral olfactory sensory neurons appears to impair odor discrimination (Albers, et al., 2006, Cheng, et al., 2013), deposition in more central olfactory areas has been shown to have little impact on olfactory performance (Phillips, et al., 2011, Vloeberghs, et al., 2008, Xu, et al., 2014). Not only was single-unit odor-evoked activity intact in LEC, but in fact, receptive field specificity of Tg2576 single-units was also comparable to WT in this area at all ages. This stands in contrast to other groups who have found a disruption of specificity in hippocampal place cells of rodent models harboring human A β PP as well as resulting spatial memory deficits (Cacucci, et al., 2008, Koistinaho, et al., 2001). Selective vulnerability of different types of neurons was previously demonstrated in two A β PP overexpressing transgenic mouse lines. While dendritic pathology was observed in a spatially defined subset of dentate granule cells prior to amyloid deposition in the PDAPP mice (Wu, et al., 2004), A β deposition induced progressive degeneration of distinct types of commissural neurons in APP23 mice (Capetillo-Zarate, et al., 2006). It is possible that the spared function seen in LEC compared to hippocampus is due to a selective vulnerability of the latter region to human A β PP and its associated metabolites (Baliatti, et al., 2013), or more robust cortical encoding of odors in the face of this pathology.

The early appearance of LEC hyperexcitability occurred prior to the detectable deposition of A β in the LEC, or in any upstream olfactory structure examined. We had previously reported A β deposition in the OB glomerular layer as early as 3 MO (Wesson, et al., 2010); however, this was not observed here. This may reflect a difference in Tg2576 cohorts or non-specific staining in the earlier report. Here we show that A β accumulation is initially detected by Western blot analysis at 12 MO selectively in the aPCX and LEC (Fig. 6A). Regardless, the lack of detectable A β deposition at ages when hyperexcitability first appears introduces the possibility that the presence of human A β PP and/or its metabolites at pre-depositing ages had an impact on LEC activity beyond that of A β plaques. In fact, the overexpression of human A β PP in olfactory sensory neurons has been shown to lead to apoptosis and changes in neuronal morphology (Cheng, et al., 2013, Cheng, et al., 2011). For example, other A β PP metabolites such as A β PP-CTFs and soluble A β PP have been shown to induce neurotoxicity, cell death and resulting memory loss (Bach, et al., 2001, Bertrand, et al., 2001, Devi and Ohno, 2012, Dewachter, et al., 2002, Deyts, et al., 2012, Lu, et al., 2000, McPhie, et al., 2001, Sopher, et al., 1994, Tamayev and D'Adamio, 2012, Tamayev, et al., 2012, Yankner, et al., 1989). Our present results demonstrate high levels of A β PP-CTFs in neurons in brain regions corresponding to the olfactory pathway, with higher levels in the aPCX than in

HPX, LEC, and OB, and the lowest found in the cerebellum. Similar relative levels were observed by ELISA for A β in the same brain regions. This difference in both A β PP-CTFs and A β levels occurs already at 3 months of age. The highest levels of both soluble A β and A β PP-CTFs in the aPCX suggests that the LEC hyperactivity in both local field potential and single-unit spontaneous activity may be induced by direct input from the piriform cortex. These data suggest a difference in the level of A β PP processing or clearance of A β PP metabolites in different brain regions, generating different levels of A β PP-CTF as well as A β . Therefore, while the prevention of A β deposition or the enhancement of A β degradation may serve to alleviate certain olfactory deficits (Cramer, et al., 2012, Morales-Corraliza, et al., 2013, Wesson, et al., 2011), attention must be paid to other metabolites of A β PP that may also exert a negative impact on normal neuronal functioning.

Acknowledgments

The authors thank Dr. Benjamin Sadrian for assistance with statistical analyses, Ivonne Lozano for performing ELISA, and Dr. Jose Morales-Corraliza and Dr. Paul M. Mathews for advice on ELISA. The work was funded by grant R01-AG037693 to EL, RAN and DAW from the National Institute of Aging.

References

1. Albers MW, Tabert MH, Devanand DP. Olfactory dysfunction as a predictor of neurodegenerative disease. *Current Neurology and Neuroscience Reports*. 2006; 6:379–386. [PubMed: 16928347]
2. Bach JH, Chae HS, Rah JC, Lee MW, Park CH, Choi SH, Choi JK, Lee SH, Kim YS, Kim KY, Lee WB, Suh YH, Kim SS. C-terminal fragment of amyloid precursor protein induces astrocytosis. *Journal of Neurochemistry*. 2001; 78:109–120. [PubMed: 11432978]
3. Bahar-Fuchs A, Moss S, Rowe C, Savage G. Awareness of olfactory deficits in healthy aging, amnesic mild cognitive impairment and Alzheimer's disease. *International Psychogeriatrics*. 2011; 23:1097–1106. [PubMed: 21251352]
4. Baliotti M, Giorgetti B, Casoli T, Solazzi M, Tamagnini F, Burattini C, Aicardi G, Fattoretti P. Early selective vulnerability of synapses and synaptic mitochondria in the hippocampal CA1 region of the Tg2576 mouse model of Alzheimer's disease. *Journal of Alzheimer's Disease*. 2013; 34:887–896.
5. Barnes DC, Hofacer RD, Zaman AR, Rennaker RL, Wilson DA. Olfactory perceptual stability and discrimination. *Nature Neuroscience*. 2008; 11:1378–1380.
6. Berens P. CircStat: A MATLAB toolbox for circular statistics. *Journal of Statistical Software*. 2009; 31:1–21.
7. Bertrand E, Brouillet E, Caille I, Bouillot C, Cole GM, Prochiantz A, Allinquant B. A short cytoplasmic domain of the amyloid precursor protein induces apoptosis in vitro and in vivo. *Mol Cell Neurosci*. 2001; 18:503–511. [PubMed: 11922141]
8. Boisselier L, Ferry B, Gervais R. Involvement of the lateral entorhinal cortex for the formation of cross-modal olfactory-tactile associations in the rat. *Hippocampus*. 2014; 24:877–891. [PubMed: 24715601]
9. Braak H, Braak E. Evolution of the neuropathology of Alzheimer's disease. *Acta Neurologica Scandinavica Supplementum*. 1996; 165:3–12. [PubMed: 8740983]
10. Braak H, Thal DR, Ghebremedhin E, Del Tredici K. Stages of the pathologic process in Alzheimer disease: Age categories from 1 to 100 years. *Journal of Neuro pathology and Experimental Neurology*. 2011; 70:960–969. [PubMed: 22002422]
11. Busche MA, Chen X, Henning HA, Reichwald J, Staufenbiel M, Sakmann B, Konnerth A. Critical role of soluble amyloid-beta for early hippocampal hyperactivity in a mouse model of Alzheimer's disease. *Proc Natl Acad Sci U S A*. 2012; 109:8740–8745. [PubMed: 22592800]

12. Busche MA, Eichhoff G, Adelsberger H, Abramowski D, Wiederhold KH, Haass C, Staufenbiel M, Konnerth A, Garaschuk O. Clusters of hyperactive neurons near amyloid plaques in a mouse model of Alzheimer's disease. *Science*. 2008; 321:1686–1689. [PubMed: 18802001]
13. Cacucci F, Yi M, Wills TJ, Chapman P, O'Keefe J. Place cell firing correlates with memory deficits and amyloid plaque burden in Tg2576 Alzheimer mouse model. *Proc Natl Acad Sci U S A*. 2008; 105:7863–7868. [PubMed: 18505838]
14. Calhoun-Haney R, Murphy C. Apolipoprotein epsilon4 is associated with more rapid decline in odor identification than in odor threshold or Dementia Rating Scale scores. *Brain Cogn*. 2005; 58:178–182. [PubMed: 15919549]
15. Cao L, Schrank BR, Rodriguez S, Benz EG, Moulia TW, Rickenbacher GT, Gomez AC, Levites Y, Edwards SR, Golde TE, Hyman BT, Barnea G, Albers MW. Abeta alters the connectivity of olfactory neurons in the absence of amyloid plaques in vivo. *Nature Communications*. 2012; 3:1009.
16. Capetillo-Zarate E, Staufenbiel M, Abramowski D, Haass C, Escher A, Stadelmann C, Yamaguchi H, Wiestler OD, Thal DR. Selective vulnerability of different types of commissural neurons for amyloid beta-protein-induced neurodegeneration in APP23 mice correlates with dendritic tree morphology. *Brain : a journal of neurology*. 2006; 129:2992–3005. [PubMed: 16844716]
17. Cavanagh C, Colby-Milley J, Bouvier D, Farso M, Chabot JG, Quirion R, Krantic S. betaCTF-correlated burst of hippocampal TNFalpha occurs at a very early, pre-plaque stage in the TgCRND8 mouse model of Alzheimer's disease. *Journal of Alzheimer's disease*. 2013; 36:233–238.
18. Chapuis J, Cohen Y, He X, Zhang Z, Jin S, Xu F, Wilson DA. Lateral entorhinal modulation of piriform cortical activity and fine odor discrimination. *The Journal of Neuroscience*. 2013; 33:13449–13459. [PubMed: 23946403]
19. Chapuis J, Wilson DA. Bidirectional plasticity of cortical pattern recognition and behavioral sensory acuity. *Nature Neuroscience*. 2012; 15:155–161.
20. Chen CF, Barnes DC, Wilson DA. Generalized vs. stimulus-specific learned fear differentially modifies stimulus encoding in primary sensory cortex of awake rats. *Journal of Neurophysiology*. 2011; 106:3136–3144. [PubMed: 21918001]
21. Cheng N, Bai L, Steuer E, Belluscio L. Olfactory functions scale with circuit restoration in a rapidly reversible Alzheimer's disease model. *The Journal of Neuroscience*. 2013; 33:12208–12217. [PubMed: 23884929]
22. Cheng N, Cai H, Belluscio L. In vivo olfactory model of APP-induced neurodegeneration reveals a reversible cell-autonomous function. *The Journal of Neuroscience*. 2011; 31:13699–13704. [PubMed: 21957232]
23. Christen-Zaech S, Kraftsik R, Pillevuit O, Kiraly M, Martins R, Khalili K, Miklossy J. Early olfactory involvement in Alzheimer's disease. *The Canadian Journal of Neurological Sciences*. 2003; 30:20–25. [PubMed: 12619779]
24. Cleland TA, Linster C. Central olfactory structures. *Handbook of Olfaction and Gustation*. 2003:165–180.
25. Conti MZ, Vicini-Chilovi B, Riva M, Zanetti M, Liberini P, Padovani A, Rozzini L. Odor identification deficit predicts clinical conversion from mild cognitive impairment to dementia due to Alzheimer's disease. *Arch Clin Neuropsychol*. 2013; 28:391–399. [PubMed: 23669447]
26. Cramer PE, Cirrito JR, Wesson DW, Lee CY, Karlo JC, Zinn AE, Casali BT, Restivo JL, Goebel WD, James MJ, Brunden KR, Wilson DA, Landreth GE. ApoE-Directed Therapeutics Rapidly Clear beta-Amyloid and Reverse Deficits in AD Mouse Models. *Science*. 2012; 335:1503–1506. [PubMed: 22323736]
27. Cummings BJ, Cotman CW. Image analysis of beta-amyloid load in Alzheimer's disease and relation to dementia severity. *Lancet*. 1995; 346:1524–1528. [PubMed: 7491048]
28. Devanand DP, Liu X, Tabert MH, Pradhaban G, Cuasay K, Bell K, de Leon MJ, Doty RL, Stern Y, Pelton GH. Combining early markers strongly predicts conversion from mild cognitive impairment to Alzheimer's disease. *Biological Psychiatry*. 2008; 64:871–879. [PubMed: 18723162]
29. Devanand DP, Michaels-Marston KS, Liu X, Pelton GH, Padilla M, Marder K, Bell K, Stern Y, Mayeux R. Olfactory deficits in patients with mild cognitive impairment predict Alzheimer's

- disease at follow-up. *The American Journal of Psychiatry*. 2000; 157:1399–1405. [PubMed: 10964854]
30. Devi L, Ohno M. Mitochondrial dysfunction and accumulation of the beta-secretase-cleaved C-terminal fragment of APP in Alzheimer's disease transgenic mice. *Neurobiol Dis*. 2012; 45:417–424. [PubMed: 21933711]
 31. Dewachter I, Reverse D, Caluwaerts N, Ris L, Kuiperi C, Van den Haute C, Spittaels K, Umans L, Serneels L, Thiry E, Moechars D, Mercken M, Godaux E, Van Leuven F. Neuronal deficiency of presenilin 1 inhibits amyloid plaque formation and corrects hippocampal long-term potentiation but not a cognitive defect of amyloid precursor protein [V717I] transgenic mice. *The Journal of Neuroscience*. 2002; 22:3445–3453. [PubMed: 11978821]
 32. Deyts C, Vetrivel KS, Das S, Shepherd YM, Dupre DJ, Thinakaran G, Parent AT. Novel GalphaS-protein signaling associated with membrane-tethered amyloid precursor protein intracellular domain. *The Journal of neuroscience*. 2012; 32:1714–1729. [PubMed: 22302812]
 33. Ferry B, Oberling P, Jarrard LE, Di Scala G. Facilitation of conditioned odor aversion by entorhinal cortex lesions in the rat. *Behavioral Neuroscience*. 1996; 110:443–450. [PubMed: 8888989]
 34. Frasnelli J, Lundstrom JN, Boyle JA, Djordjevic J, Zatorre RJ, Jones-Gotman M. Neuroanatomical correlates of olfactory performance. *Experimental Brain Research*. 2010; 201:1–11. [PubMed: 19730837]
 35. Goutagny R, Gu N, Cavanagh C, Jackson J, Chabot JG, Quirion R, Krantic S, Williams S. Alterations in hippocampal network oscillations and theta-gamma coupling arise before Abeta overproduction in a mouse model of Alzheimer's disease. *Eur J Neurosci*. 2013; 37:1896–1902. [PubMed: 23773058]
 36. Guerin D, Sacquet J, Mandairon N, Jourdan F, Didier A. Early locus coeruleus degeneration and olfactory dysfunctions in Tg2576 mice. *Neurobiology of Aging*. 2009; 30:272–283. [PubMed: 17618708]
 37. Hardy JA, Higgins GA. Alzheimer's disease: the amyloid cascade hypothesis. *Science*. 1992; 256:184–185. [PubMed: 1566067]
 38. Igarashi KM, Ieki N, An M, Yamaguchi Y, Nagayama S, Kobayakawa K, Kobayakawa R, Tanifuji M, Sakano H, Chen WR, Mori K. Parallel mitral and tufted cell pathways route distinct odor information to different targets in the olfactory cortex. *Journal of Neuroscience*. 2012; 32:7970–7985. [PubMed: 22674272]
 39. Ittner LM, Gotz J. Amyloid-beta and tau--a toxic pas de deux in Alzheimer's disease. *Nat Rev Neurosci*. 2011; 12:65–72. [PubMed: 21193853]
 40. Jiang Y, Mullaney KA, Peterhoff CM, Che S, Schmidt SD, Boyer-Boiteau A, Ginsberg SD, Cataldo AM, Mathews PM, Nixon RA. Alzheimer's-related endosome dysfunction in Down syndrome is Abeta-independent but requires APP and is reversed by BACE-1 inhibition. *Proc Natl Acad Sci U S A*. 2010; 107:1630–1635. [PubMed: 20080541]
 41. Kaye R, Head E, Thompson JL, McIntire TM, Milton SC, Cotman CW, Glabe CG. Common structure of soluble amyloid oligomers implies common mechanism of pathogenesis. *Science*. 2003; 300:486–489. [PubMed: 12702875]
 42. Koistinaho M, Ort M, Cimadevilla JM, Vondrous R, Cordell B, Koistinaho J, Bures J, Higgins LS. Specific spatial learning deficits become severe with age in beta-amyloid precursor protein transgenic mice that harbor diffuse beta-amyloid deposits but do not form plaques. *Proc Natl Acad Sci U S A*. 2001; 98:14675–14680. [PubMed: 11724968]
 43. Lacor PN, Buniel MC, Chang L, Fernandez SJ, Gong Y, Viola KL, Lambert MP, Velasco PT, Bigio EH, Finch CE, Krafft GA, Klein WL. Synaptic targeting by Alzheimer's-related amyloid beta oligomers. *The Journal of neuroscience : the official journal of the Society for Neuroscience*. 2004; 24:10191–10200. [PubMed: 15537891]
 44. Lauritzen I, Pardossi-Piquard R, Bauer C, Brigham E, Abraham JD, Ranaldi S, Fraser P, St-George-Hyslop P, Le Thuc O, Espin V, Chami L, Dunys J, Checler F. The beta-secretase-derived C-terminal fragment of betaAPP, C99, but not Abeta, is a key contributor to early intraneuronal lesions in triple-transgenic mouse hippocampus. *The Journal of Neuroscience*. 2012; 32:16243–16255a. [PubMed: 23152608]

45. Lovitz AM, Sloan AM, Rennaker RL, Wilson DA. Complex mixture discrimination and the role of contaminants. *Chemical Senses*. 2012; 37:533–540. [PubMed: 22354907]
46. Lu DC, Rabizadeh S, Chandra S, Shayya RF, Ellerby LM, Ye X, Salvesen GS, Koo EH, Bredesen DE. A second cytotoxic proteolytic peptide derived from amyloid beta-protein precursor. *Nature Medicine*. 2000; 6:397–404.
47. McPhie DL, Golde T, Eckman CB, Yager D, Brant JB, Neve RL. beta-Secretase cleavage of the amyloid precursor protein mediates neuronal apoptosis caused by familial Alzheimer's disease mutations. *Brain Res Mol Brain Res*. 2001; 97:103–113. [PubMed: 11744168]
48. Morales-Corraliza J, Mazzella MJ, Berger JD, Diaz NS, Choi JH, Levy E, Matsuoka Y, Planel E, Mathews PM. In vivo turnover of tau and APP metabolites in the brains of wild-type and Tg2576 mice: greater stability of sAPP in the beta-amyloid depositing mice. *PloS one*. 2009; 4:e7134. [PubMed: 19771166]
49. Morales-Corraliza J, Schmidt SD, Mazzella MJ, Berger JD, Wilson DA, Wesson DW, Jucker M, Levy E, Nixon RA, Mathews PM. Immunization targeting a minor plaque constituent clears beta-amyloid and rescues behavioral deficits in an Alzheimer's disease mouse model. *Neurobiology of Aging*. 2013; 34:137–145. [PubMed: 22608241]
50. Mouly AM, Di Scala G. Entorhinal cortex stimulation modulates amygdala and piriform cortex responses to olfactory bulb inputs in the rat. *Neuroscience*. 2006; 137:1131–1141. [PubMed: 16325349]
51. Murphy C. Loss of olfactory function in dementing disease. *Physiology & Behavior*. 1999; 66:177–182. [PubMed: 10336141]
52. Murphy C, Schubert CR, Cruickshanks KJ, Klein BE, Klein R, Nondahl DM. Prevalence of olfactory impairment in older adults. *JAMA : the Journal of the American Medical Association*. 2002; 288:2307–2312.
53. Nhan HS, Chiang K, Koo EH. The multifaceted nature of amyloid precursor protein and its proteolytic fragments: friends and foes. *Acta Neuropathol*. 2014
54. Nordin S, Murphy C. Odor memory in normal aging and Alzheimer's disease. *Annals of the New York Academy of Sciences*. 1998; 855:686–693. [PubMed: 9929672]
55. Phillips M, Boman E, Osterman H, Willhite D, Laska M. Olfactory and visuospatial learning and memory performance in two strains of Alzheimer's disease model mice—a longitudinal study. *PloS one*. 2011; 6:e19567. [PubMed: 21573167]
56. Rahayel S, Frasnelli J, Joubert S. The effect of Alzheimer's disease and Parkinson's disease on olfaction: a meta-analysis. *Behavioural Brain Research*. 2012; 231:60–74. [PubMed: 22414849]
57. Selkoe DJ. Alzheimer's disease: a central role for amyloid. *J Neuropathol Exp Neurol*. 1994; 53:438–447. [PubMed: 8083687]
58. Sopher BL, Fukuchi K, Smith AC, Leppig KA, Furlong CE, Martin GM. Cytotoxicity mediated by conditional expression of a carboxyl-terminal derivative of the beta-amyloid precursor protein. *Brain Res Mol Brain Res*. 1994; 26:207–217. [PubMed: 7854049]
59. Staubli U, Ivy G, Lynch G. Hippocampal denervation causes rapid forgetting of olfactory information in rats. *Proc Natl Acad Sci U S A*. 1984; 81:5885–5887. [PubMed: 6592592]
60. Tamayev R, D'Adamio L. Inhibition of gamma-secretase worsens memory deficits in a genetically congruous mouse model of Danish dementia. *Mol Neurodegener*. 2012; 7:19. [PubMed: 22537414]
61. Tamayev R, Matsuda S, Arancio O, D'Adamio L. beta- but not gamma-secretase proteolysis of APP causes synaptic and memory deficits in a mouse model of dementia. *EMBO Mol Med*. 2012; 4:171–179. [PubMed: 22170863]
62. Upadhaya AR, Lungrin I, Yamaguchi H, Fandrich M, Thal DR. High-molecular weight Abeta oligomers and protofibrils are the predominant Abeta species in the native soluble protein fraction of the AD brain. *J Cell Mol Med*. 2012; 16:287–295. [PubMed: 21418518]
63. Vloeberghs E, Van Dam D, Franck F, Serroyen J, Geert M, Staufenbiel M, De Deyn PP. Altered ingestive behavior, weight changes, and intact olfactory sense in an APP overexpression model. *Behavioral Neuroscience*. 2008; 122:491–497. [PubMed: 18513119]
64. Walsh DM, Hartley DM, Kusumoto Y, Fezoui Y, Condron MM, Lomakin A, Benedek GB, Selkoe DJ, Teplow DB. Amyloid beta-protein fibrillogenesis. Structure and biological activity of

- protofibrillar intermediates. *The Journal of Biological Chemistry*. 1999; 274:25945–25952. [PubMed: 10464339]
65. Walsh DM, Lomakin A, Benedek GB, Condron MM, Teplow DB. Amyloid beta-protein fibrillogenesis. Detection of a protofibrillar intermediate. *The Journal of Biological Chemistry*. 1997; 272:22364–22372. [PubMed: 9268388]
66. Walsh DM, Selkoe DJ. A-beta oligomers - a decade of discovery. *Journal of Neurochemistry*. 2007; 101:1172–1184. [PubMed: 17286590]
67. Wesson DW, Borkowski AH, Landreth GE, Nixon RA, Levy E, Wilson DA. Sensory network dysfunction, behavioral impairments, and their reversibility in an Alzheimer's beta-amyloidosis mouse model. *The Journal of Neuroscience*. 2011; 31:15962–15971. [PubMed: 22049439]
68. Wesson DW, Levy E, Nixon RA, Wilson DA. Olfactory dysfunction correlates with amyloid-beta burden in an Alzheimer's disease mouse model. *The Journal of Neuroscience*. 2010; 30:505–514. [PubMed: 20071513]
69. Wilson DA, Stevenson RJ. Olfactory perceptual learning: the critical role of memory in odor discrimination. *Neuroscience and Biobehavioral Reviews*. 2003; 27:307–328. [PubMed: 12946684]
70. Wilson DA, Sullivan RM. Cortical processing of odor objects. *Neuron*. 2011; 72:506–519. [PubMed: 22099455]
71. Wilson DA, Xu W, Sadrian B, Courtiol E, Cohen Y, Barnes DC. Cortical odor processing in health and disease. *Prog Brain Res*. 2014; 208:275–305. [PubMed: 24767487]
72. Wirth S, Ferry B, Di Scala G. Facilitation of olfactory recognition by lateral entorhinal cortex lesion in rats. *Behavioural Brain Research*. 1998; 91:49–59. [PubMed: 9578439]
73. Wu CC, Chawla F, Games D, Rydel RE, Freedman S, Schenk D, Young WG, Morrison JH, Bloom FE. Selective vulnerability of dentate granule cells prior to amyloid deposition in PDAPP mice: digital morphometric analyses. *Proc Natl Acad Sci U S A*. 2004; 101:7141–7146. [PubMed: 15118092]
74. Xu F, Lopez-Guzman M, Schoen C, Fitzgerald S, Lauer SL, Nixon RA, Levy E, Wilson DA. Spared piriform cortical single-unit odor processing and odor discrimination in the Tg2576 mouse model of Alzheimer's disease. *PloS one*. 2014 (in press).
75. Xu W, Wilson DA. Odor-evoked activity in the mouse lateral entorhinal cortex. *Neuroscience*. 2012; 223:12–20. [PubMed: 22871522]
76. Yankner BA, Dawes LR, Fisher S, Villa-Komaroff L, Oster-Granite ML, Neve RL. Neurotoxicity of a fragment of the amyloid precursor associated with Alzheimer's disease. *Science*. 1989; 245:417–420. [PubMed: 2474201]
77. Zheng H, Koo EH. The amyloid precursor protein: beyond amyloid. *Mol Neurodegener*. 2006; 1:5. [PubMed: 16930452]
78. Zheng H, Koo EH. Biology and pathophysiology of the amyloid precursor protein. *Mol Neurodegener*. 2011; 6:27. [PubMed: 21527012]

Highlights

- The LEC shows early hyperexcitability in a model of A β PP over-expression
- This hyperexcitability is associated with elevated A β PP metabolites in the aPCX
- Elevated A β PP metabolites in the aPCX included intracellular A β PP-CTF and soluble A β
- Both soluble A β and non-A β A β PP metabolites may promote early LEC pathology

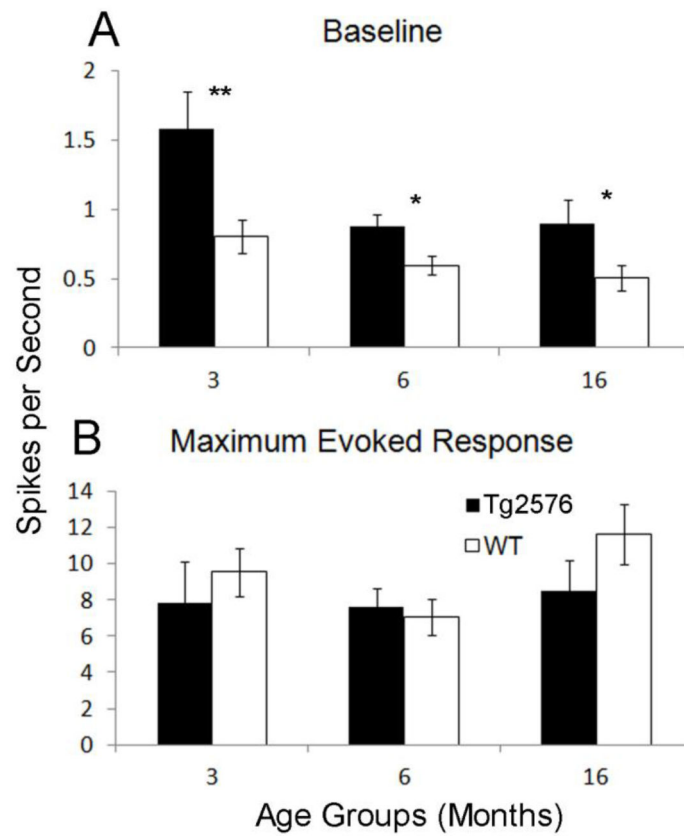


Figure 2. Baseline and maximal odor-evoked activity in lateral entorhinal cortex of Tg2576 versus age-matched WT mice. Solid bars represent Tg2576 while open bars represent WT. Baseline (A) activity was significantly elevated in 3, 6 and 16 MO Tg2576 versus age matched WT animals. Meanwhile, a comparison of the maximal odor-evoked firing rate (A) of Tg2576 versus WT revealed no differences at any age. ** = $p < .01$, * = $p < .05$.

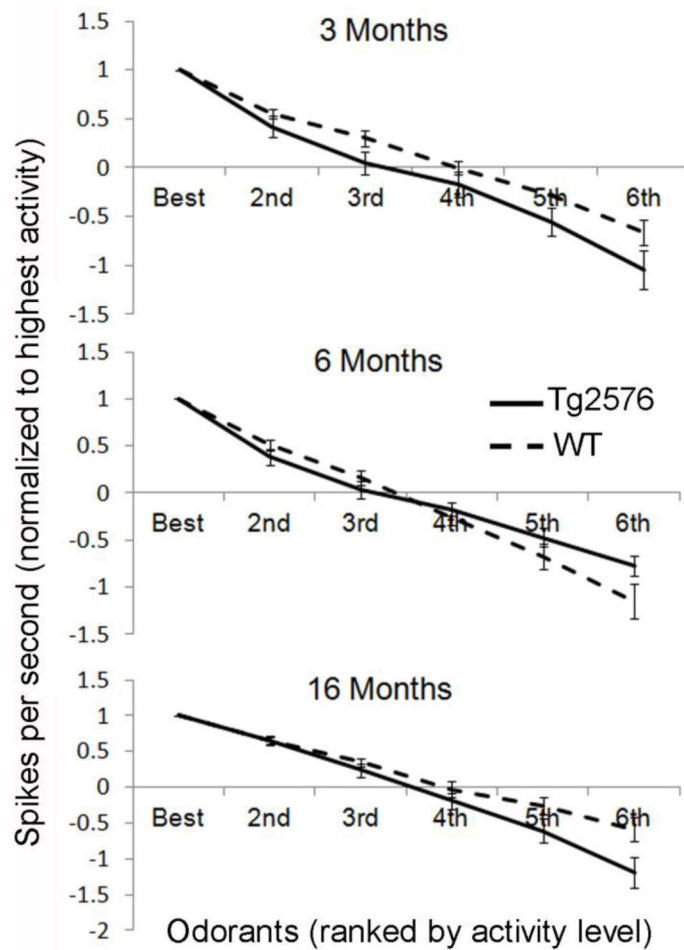


Figure 3. Olfactory receptive fields in lateral entorhinal cortex of Tg2576 versus age-matched WT mice. Receptive fields are calculated by ranking odor-evoked spike activity from highest to lowest (6th). Spikes per second is then normalized to the highest firing rate, creating a gradient of activity in response to each different odor. Receptive field activity in LEC of Tg2576 was not significantly different from WT at any age.

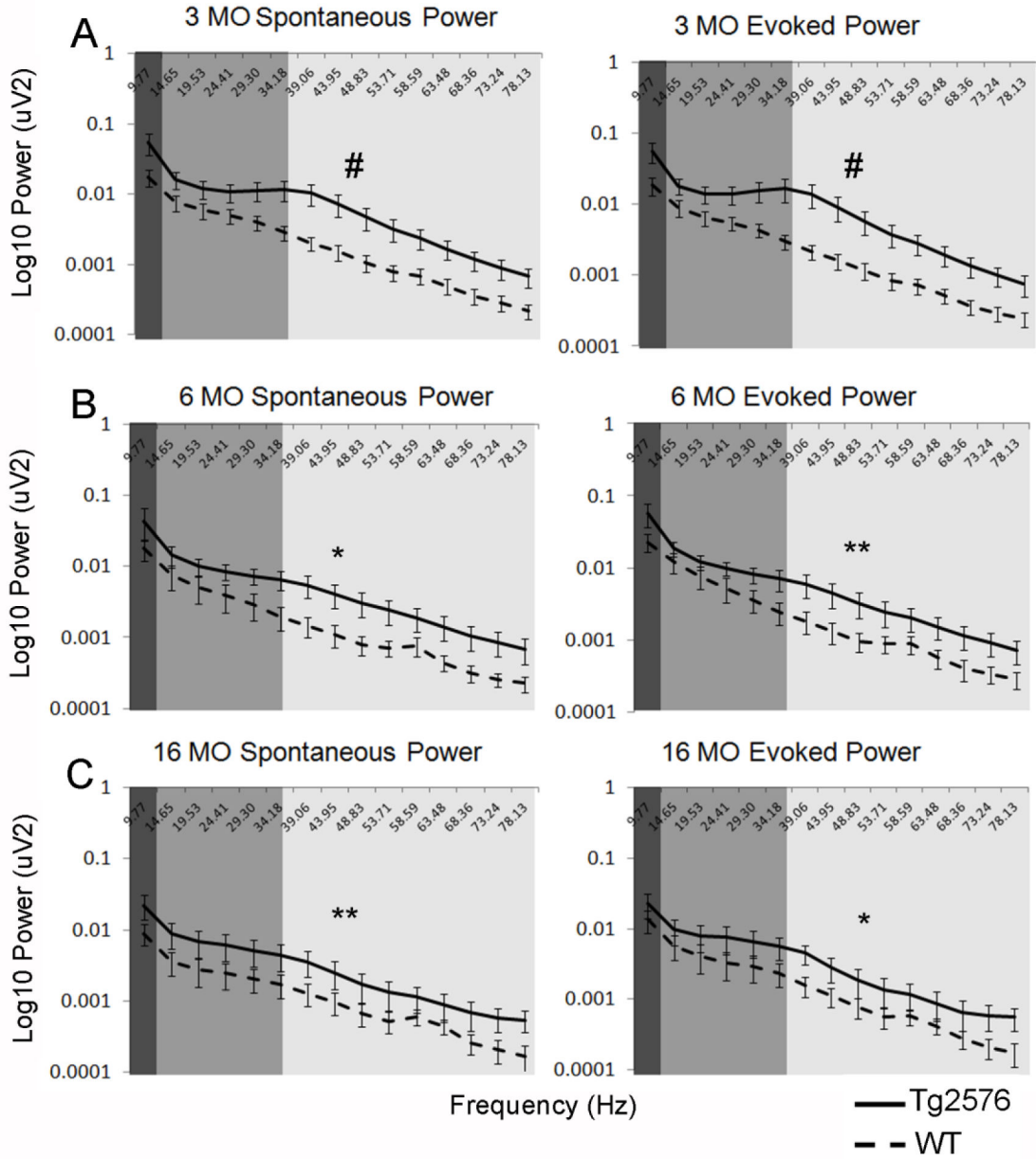


Figure 4. Spontaneous and odor-evoked LFP in lateral entorhinal cortex of Tg2576 versus age-matched WT mice. Solid lines represent Tg2576 while broken lines represent WT. In 3 (A), 6 (B) and 16 MO (C) age cohorts, Tg2576 exhibited significantly elevated baseline as well as odor-evoked LFPs across the theta (dark gray), beta (medium gray) and gamma (light gray) frequency ranges. # = $p < .0001$, ** = $p < .0005$, * = $p < .005$

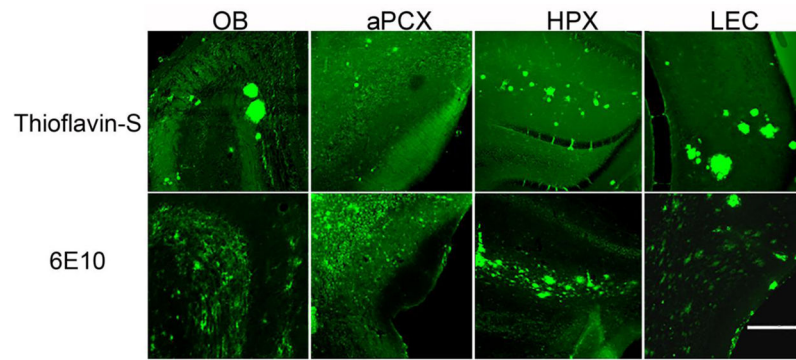


Figure 5. A β plaque deposition in the OB, PCX, HPX and LEC of 16 MO Tg2576 mice demonstrated by thioflavin S staining and both fibrillar and non fibrillar A β accumulation in the same regions revealed by 6E10 immunolabeling. Scale bar = 200 μ m.

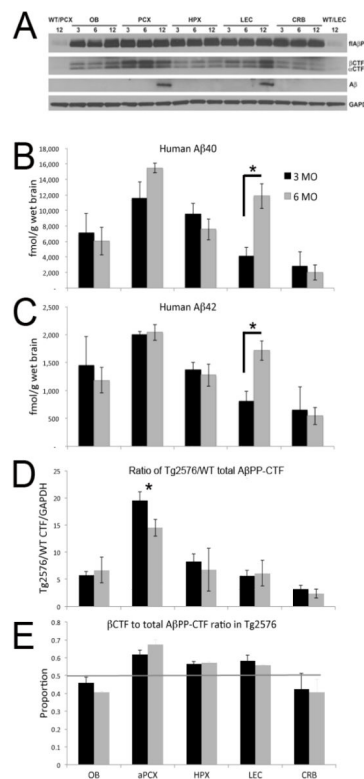


Figure 6. Western blot and ELISA of flAβPP, AβPP-CTF, and Aβ in OB, PCX, HPX, LEC and CRB of Tg2576 mice. (A) Western blots with C1/6.1 antibody show flAβPP overexpression as well as both αCTF and βCTF in 3, 6, and 12 MO Tg2576 OB, PCX, HPX, LEC and cerebellum (CRB). While at 3 and 6 MO, there is no Aβ accumulation as shown using 4G8 antibody, Aβ accumulates at 12 MO in the PCX and LEC, but not in the OB, HPX, and CRB. ELISA of Aβ40 (B) and Aβ42 (C) in the brain of 3 and 6 MO Tg2576 mice. Asterisks signify significant difference between 3 MO and 6 MO levels in LEC. Quantification of total AβPP-CTFs, including both αCTF and βCTF, shows highest levels in PCX (D) at 3 and 6 MO, as observed for Aβ40 and Aβ42. Asterisk signifies a significant difference between aPCX levels compared to all other regions. There was no significant effect of age. The ratio of βCTF to total AβPP-CTFs was compared in 3 and 6 MO Tg2576 in all brain areas (E). Line shows a ratio of 0.50. Bars above the line indicate the majority of AβPP-CTF detected was βCTF. Bars below the line indicate the majority of AβPP-CTF detected was αCTF. In contrast to OB and CRB where αCTF predominated, the majority of AβPP-CTFs in PCX, HPX and LEC were of the β form. See text for statistical analyses. Error bars indicate 1 SE.

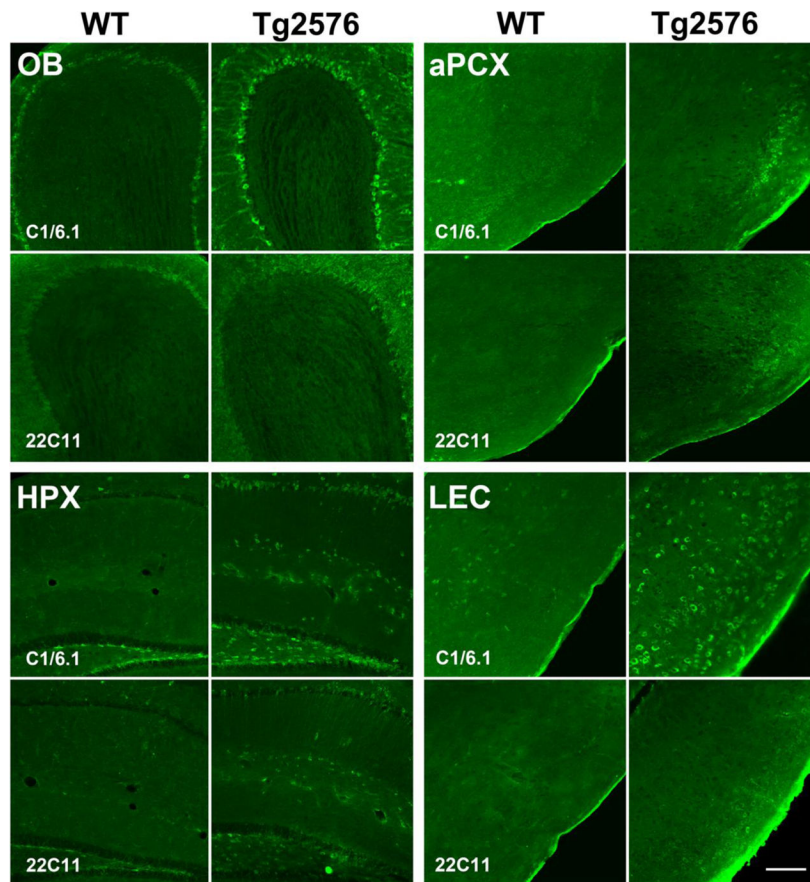


Figure 7. Representative 6 MO immunohistochemistry for A β PP-CTFs (C1/6.1) and flA β PP (22C11) in OB, aPCX, HPX and LEC of Tg2576 versus WT mice. Tg2576 showed elevated C1/6.1 staining compared to WT which suggests an accumulation of A β PP-CTFs. Elevation is seen also in sections treated with 22C11 but to a lesser extent than those treated with C1/6.1. Scale bar = 200 μ m.